

# Light-Induced Structural Transformation in Self-Assembled Monolayer of 4-(Amyloxy)cinnamic Acid Investigated with Scanning Tunneling Microscopy

Li-Ping Xu,<sup>†</sup> Cun-Ji Yan,<sup>†</sup> Li-Jun Wan,\* Si-Guang Jiang,<sup>†</sup> and Ming-Hua Liu

*Institute of Chemistry, Chinese Academy of Sciences (CAS), Beijing 100080, P. R. China*

*Received: June 3, 2005; In Final Form: June 29, 2005*

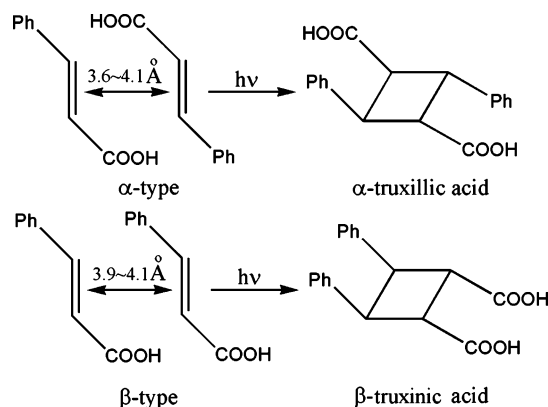
UV light irradiation effect on the structural transformation in a self-assembled monolayer of 4-(amyloxy)-cinnamic acid (AOCA) on Au(111) has been investigated by using electrochemical scanning tunneling microscopy (ECSTM), cyclic voltammetry, and infrared (IR) spectroscopy. A well-defined 4-(amyloxy)-cinnamic acid adlayer with a  $(4 \times 11)$  symmetry was first prepared on Au(111). After UV-light irradiation onto the adlayer, a new adlayer is observed with different molecular arrangement and a symmetry of  $(5 \times 8)$ . On the basis of the results from high-resolution STM image and photochemical reaction, a dimerization of AOCA molecules in the adlayer with structural transformation is concluded. Schematic models have been proposed for the unirradiated and irradiated adlayers, respectively. The direct evidence at molecular level about photodimerization of cinnamic acid on metal substrate is presented.

## Introduction

Self-assembling is a critical and necessary process in living organisms and of ever-increasing importance in chemistry and material science.<sup>1–3</sup> Now this process plays an important role in the so-called “bottom-up” strategy for nanofabrication. Because self-assembled monolayers (SAMs) with controlled structure and function are promising candidates,<sup>1–3</sup> the control of two-dimensional molecular arrangement is the prerequisite for their potential application in nanodevice development. Therefore, understanding the structural transformation on a SAM is an important issue in the study of surface molecular patterning. It is well-known that the structure of a SAM depends on the chemical structure of the molecules used in the SAM. However, light irradiation becomes a facile method to tune SAM's structure as a simple external stimulus like other methods of heating and electric and/or magnetic fields.<sup>4–7</sup> Photochemical reaction occurring within the monolayer of photoactive molecules has been investigated by the techniques such as UV–vis absorption spectroscopy, surface fluorescence and FTIR,<sup>8–10</sup> providing average structural information.

Owing to the advantage with well-established scanning tunneling microscopy (STM), it has been intensively used to study the molecular ordering, dynamics, and chemical process in SAMs.<sup>11,12</sup> The light-induced changes in photochemical reactive adlayers at highly oriented pyrolytic graphite (HOPG) surface were investigated previously.<sup>13–19</sup> For example, by imaging the starting material and the reaction product of a reversible photoreaction, Schryver et al. studied the cis–trans isomerization of azobenzene derivatives.<sup>13</sup> After UV irradiation was applied onto a well-defined self-assembled monolayer of diacetylene monomers, the conjugated polydiacetylene nano-

SCHEME 1: Schematic Illustration of Photodimerization of AOCA in a Solid State



wires were observed.<sup>15–19</sup> However, the study of photoinduced structural transformation in a monolayer at metal surface with STM is rarely reported,<sup>20</sup> which is crucial to understand the surface chemical reaction and to develop photoresponsive and electronic nanodevices as well as novel nanomaterials.

Cinnamic acid is a typical photoreactive compound.<sup>21–22</sup> There exist three forms of the compound in its solid crystals,  $\alpha$ ,  $\beta$  and  $\gamma$ . The distances between neighboring parallel double bonds in  $\alpha$ - (head-to-tail),  $\beta$ - (head-to-head) and  $\gamma$ -type monomers are 3.6–4.1, 3.9–4.1, and 4.8–5.1 Å, respectively. The solid-state dimerization of cinnamic acid is topochemically controlled. As shown in Scheme 1, the  $\alpha$ -form of the monomers gives the dimeric product of  $\alpha$ -truxillic acid, whereas the  $\beta$ -form of the monomers produces  $\beta$ -truxinic acid, and the  $\gamma$ -form of the monomers is photostable.

Herein, we employ a derivative of cinnamic acid, 4-(amyloxy)cinnamic acid (AOCA,  $C_5H_{11}OC_6H_4CH=COOH$ ), as a model system to investigate its photoreaction process. The AOCA SAM was prepared on Au(111) surface. The structure

\* Corresponding author. Tel. & Fax: +86-10-62558934. E-mail: wanlijun@iccas.ac.cn.

<sup>†</sup> Also in CAS Graduate school.

of the as-prepared SAM was then tuned by UV light. CV, STM, and IR were used to study the photochemical reaction and the structural transition in the adlayer. A dimerization of the AOCA molecules and structural transition in the adlayer were clearly observed in STM images. The results provide direct evidence at the molecular level about photodimerization of cinnamic acid on the metal substrate and should be important in surface nanofabrication.

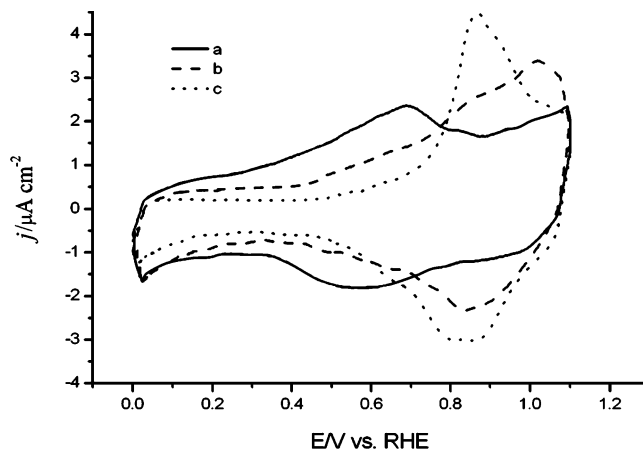
## Experimental Section

AOCA molecules were from Acros Chemicals Co. Inc. The preparation for the Au(111) crystal and electrolyte solution was the same procedure as reported in the literature.<sup>20,23,24</sup> Briefly, a well-defined Au(111) electrode was prepared by crystallization of a molten ball formed at the end of a Au wire (99.999%) in a hydrogen–oxygen flame. For cyclic voltammetric measurements, one of the (111) facets on a gold bead was mechanically polished with a successively finer grade of Al<sub>2</sub>O<sub>3</sub> and annealed at 900 °C for 24 h to remove damages on the surface. Before each measurement, the Au(111) electrode was further annealed in a hydrogen–oxygen flame and quenched in ultrapure water (Milli-Q) saturated with hydrogen. The AOCA SAM was obtained by immersing Au(111) into an ethanol solution containing 0.1 mM AOCA for 1 min. Then the Au(111) electrode was rinsed with Milli-Q ultrapure water to remove the remnant molecules and transferred into the STM electrochemical cell. The aqueous HClO<sub>4</sub> was prepared by diluting HClO<sub>4</sub> (Cica-Merck, Japan, Ultrapure grade) with Milli-Q water.

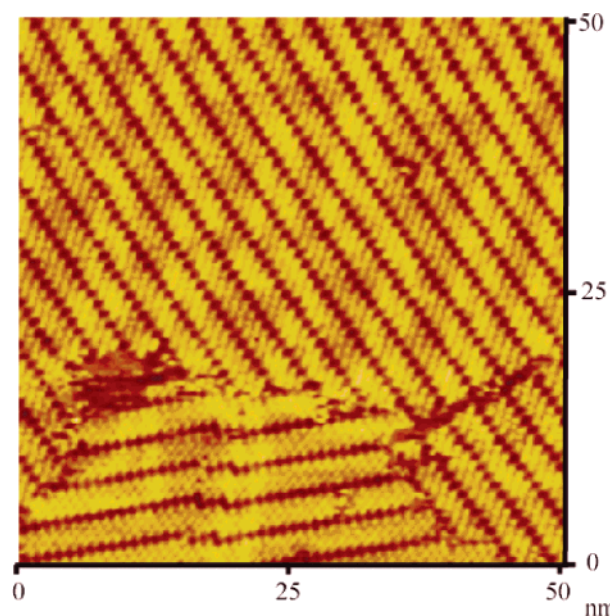
Cyclic voltammetry was carried out with the hanging meniscus method in a three-compartment electrochemical cell under a N<sub>2</sub> atmosphere. A reversible hydrogen electrode (RHE) and a platinum wire were used as the reference and counter electrodes. Electrochemical STM measurements were carried out with a Nanoscope E microscope (Digital Instrument Inc.). The STM tips used were made from electrochemically etched tungsten wire (0.25 mm in diameter) in 0.6 M KOH. To minimize faradic currents, the sidewall of the tips was sealed with clear nail polish. All images acquired in the constant-current mode to evaluate the corrugation heights of the Au(111) substrate and the adsorbed molecules. All STM images were flattened raw data without any processing such as low-pass and high-pass. The electrode potentials were reported with respect to RHE. All molecular models were optimized with Hyperchem software package (version 6.0). The infrared spectra were recorded on a FT/IR spectrophotometer (JAS. Co, FT/IR-660 plus).

## Results and Discussion

**Cyclic Voltammograms (CVs).** The electrochemical behavior of the AOCA-modified Au(111) electrode was investigated by cyclic voltammetry in 0.1 M HClO<sub>4</sub>. Figure 1 shows the CVs of bare, unirradiated and irradiated AOCA-modified Au(111) electrodes recorded at a scan rate of 30 mV s<sup>-1</sup>. The CV (line a) of the bare Au(111) in the double-layer potential region from 0 to 1.1 V is identical to that reported previously,<sup>24</sup> showing that a well-defined Au(111) surface was exposed to HClO<sub>4</sub> solution and free from contamination. Line b is the CV obtained from AOCA-modified Au(111) electrode in 0.1 M HClO<sub>4</sub>. It can be seen that the adsorption of AOCA results in the disappearance of the reconstruction peak and the decrease in the electric charge in the double-layer. A pair of peaks with a broad oxidation peak arising at 0.8 V and reduction peak at 0.83 V is observed, respectively. It can be ascribed to the electrochemical process of AOCA. After recording line b,



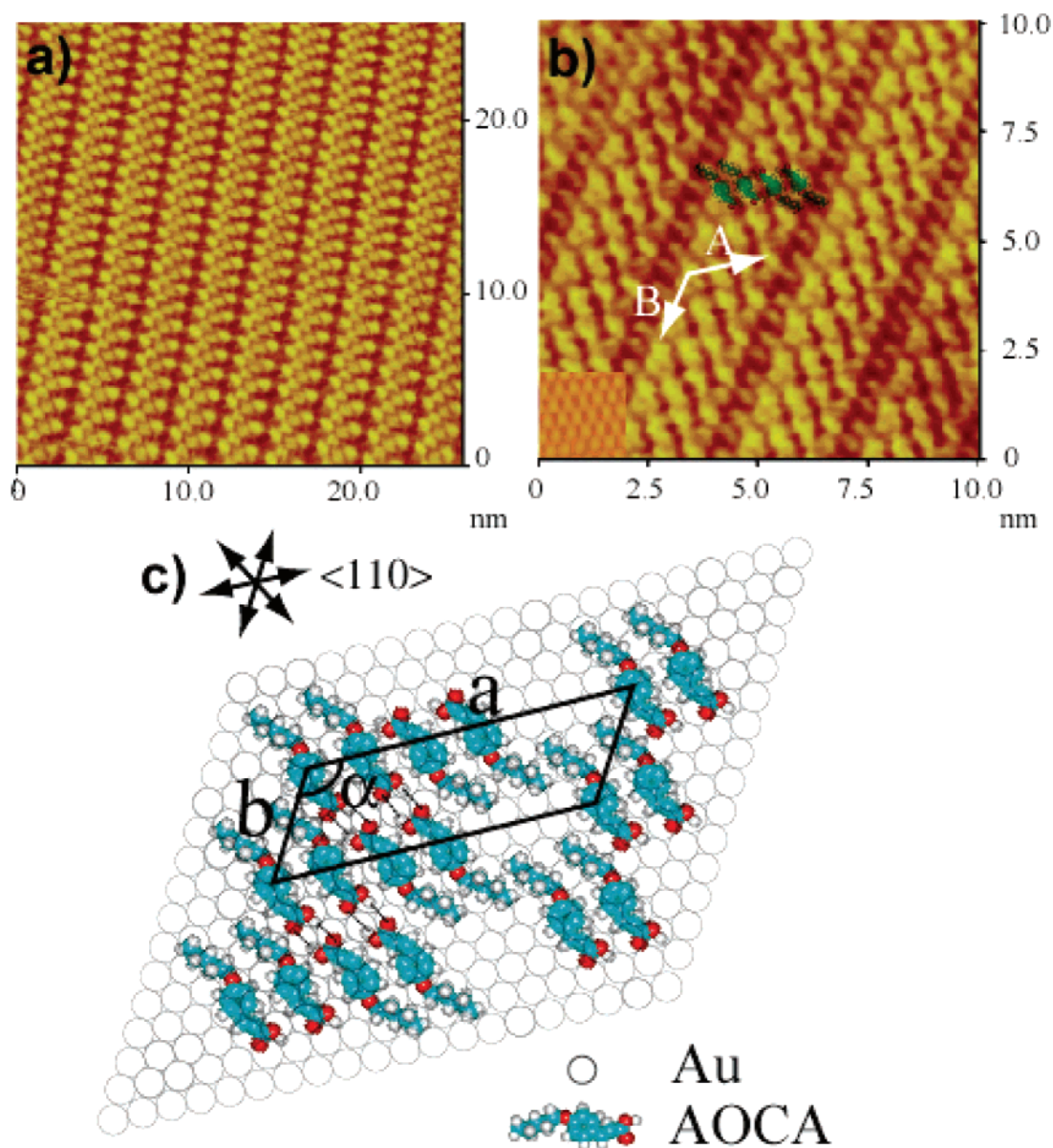
**Figure 1.** Typical cyclic voltammograms measured in 0.1 M HClO<sub>4</sub> in the potential region between 0 and 1.1 V at a scan rate of 30 mV/s: (a) bare Au(111); (b) AOCA-modified Au(111); (c) AOCA-modified Au(111) after 10 min irradiation.



**Figure 2.** STM image of AOCA adlayer with several domains on Au(111). The bias voltage and tunneling current were −100 mV and +700 pA, respectively.

the AOCA-modified Au(111) electrode was taken out from the electrochemical cell and directly irradiated by UV light (wavelength: 365 nm) for ca. 10 min. Then the electrode was put into the electrochemical cell again to measure CV. The result was shown in Figure 1 by line c. It is clear that the shape of the line c is similar with that of the line b, although the electric charges involved in the double-layer is much smaller. However, the peaks in line c are sharper than those in line b, with an increase of the total charge under the peak. This increase can be assigned to the structural difference between the monomer and dimer.

**STM of AOCA Adlayer.** The adlayer structure of AOCA was observed by STM. Figure 2 is a large scale STM image showing the structure of AOCA adlayer. This image was acquired at 0.6 V in 0.1 M HClO<sub>4</sub>. There are several molecular domains different from Au(111) substrate in the image. The molecular domains can be found crossing each other with an angle of 60° or 120°. Molecular defects exist in the domain boundaries. The results directly demonstrate that a SAM of AOCA is successfully prepared on Au(111) surface.



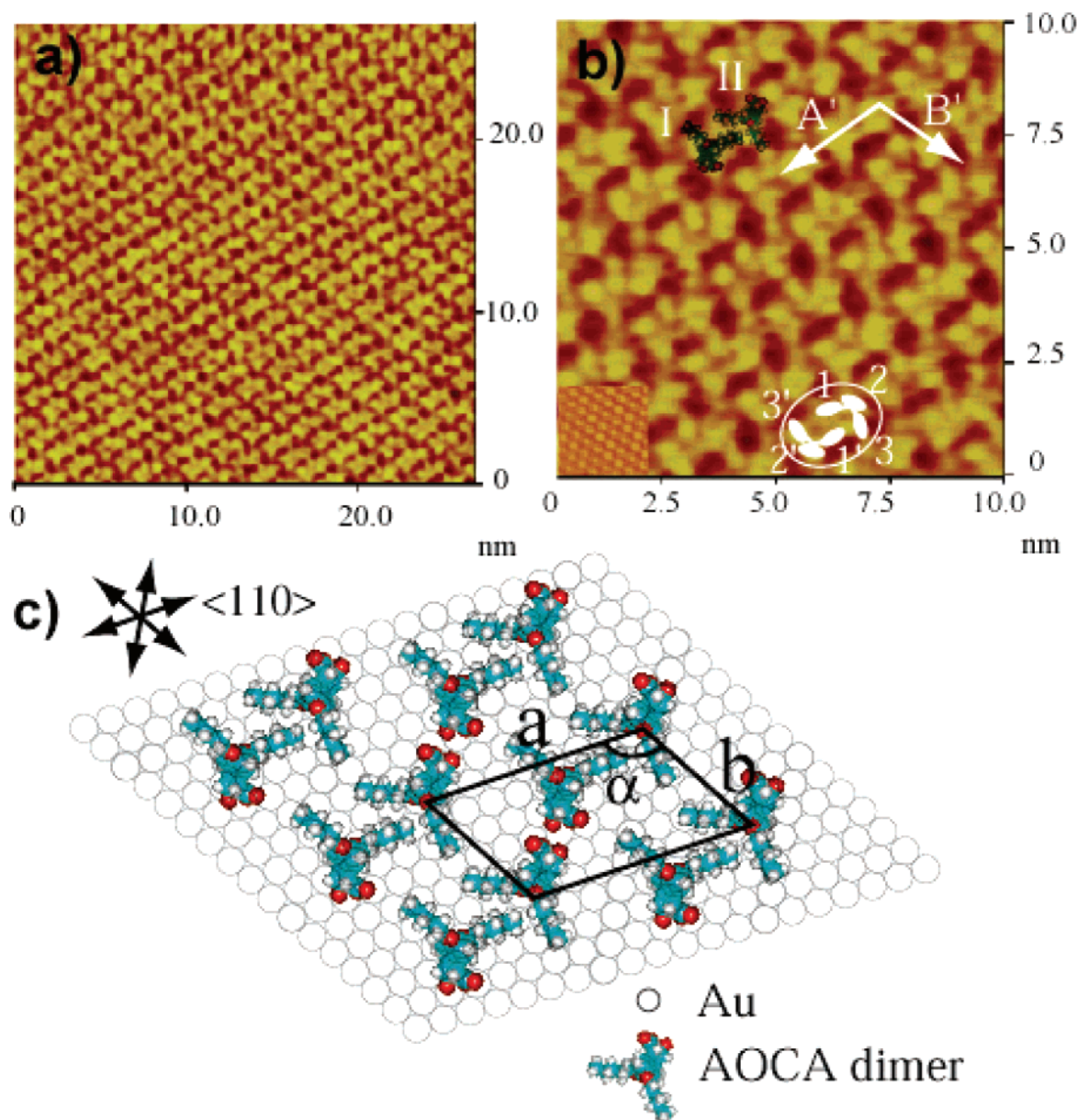
**Figure 3.** (a) Large-scale and (b) higher resolution STM images of AOCA adlayer on Au(111) with a bias voltage of  $-150$  mV and a tunneling current of  $700$  pA. An inserted STM image in (b) shows Au(111) substrate. (c) Proposed structural model for AOCA adlayer on Au(111).

Figure 3a is a typical STM image ( $25 \times 25$  nm<sup>2</sup>) acquired on an AOCA adlayer at  $0.6$  V. The SAM consisted of regular molecular rows aligning along close-packed direction of Au(111) lattice and extended over the flat terrace of the substrate surface. The structural details can be seen in a higher resolution STM image of Figure 3b. The molecular rows in **A** direction are composed of several sets of elliptical spots. Each set has four bright spots in a molecular row. After careful observation, it is found that a depression existed in the center of an individual elliptical spot. The aliphatic chains can also be identified. From the chemical structure, it is clear that an elliptical spot corresponds to the cinnamate moiety of an AOCA molecule. A schematically illustration for this molecular arrangement was drawn in Figure 3b indicating a set of four AOCA molecules. The repeated distances along **A** direction and **B** direction are measured to be  $3.16$  and  $1.15$  nm with an experimental error  $\pm 0.2$  nm, respectively. The internal angle  $\alpha$  between **A** and **B** was  $120 \pm 2^\circ$ . Both **A** and **B** directions are along  $\langle 110 \rangle$  direction by the comparison of Au(111)– $(1 \times 1)$ . Therefore, a unit cell with a  $(4 \times 11)$  symmetry for the molecular adlayer can be

concluded. A structural model is proposed in Figure 3c. The hydrogen atom in carboxyl groups can form H-bond with the oxygen atom of another carboxyl group, as indicated by dashed lines in Figure 3c, which stabilize the adsorption of AOCA monomer on Au(111).

**STM of AOCA Adlayer after UV Light Irradiation.** After the AOCA adlayer was imaged, the electrolyte solution was removed from electrochemical cell. The AOCA-modified Au electrode was irradiated with UV light (wavelength:  $365$  nm) for ca.  $10$  min to induce photochemical reaction. After the irradiation, the cell was refilled with electrolyte solution again. STM images observed after UV-light irradiation reveal a new packing pattern in the adlayer. The molecular appearance shows a quite different structure shown in Figure 4a. The image was acquired at  $0.6$  V. At first, the adlayer symmetry is changed. Although the molecular rows of **A'** and **B'** are along the  $\langle 110 \rangle$  direction and crossed each other at an angle of  $120 \pm 2^\circ$ , the repeated distances along **A'** and **B'** were measured to be  $2.30 \pm 0.2$  and  $1.44 \pm 0.2$  nm, respectively. On the basis of the molecular orientation and intermolecular distance, **A** ( $5 \times 8$ )





**Figure 4.** (a) Large scale and (b) higher resolution STM images of the AOCA dimeric adlayer on Au(111) with a bias voltage of  $-150$  mV and a tunneling current of  $700$  pA. The inserted STM image in (b) is Au(111) substrate. (c) Proposed structural model for the dimeric adlayer.

structure can be concluded. Furthermore, the structural details are revealed from the higher resolution STM image in Figure 4b. The molecular appearance and arrangement are completely different from those in Figure 3. Regular and identical trifolium-shape clusters with sets of three bright spots appear in the adlayer, indicating the occurrence of photochemical reaction in AOCA adlayer. It is noted that there are pairs of trifolium-shape clusters. For example, in the white circle indicated in the image, two trifolium-shape clusters can be seen with 6 bright spots. Compared with the chemical structure of a dimer, each “trifolium” consisting of three bright spots indicated by 1, 2 and 3, is a molecular dimer. Two dimers form a molecular pair as illustrated in Figure 4b. The three bright spots in another dimer are indicated by 1', 2' and 3'. The two dimers take an opposite arrangement in the circle. Therefore, from the chemical structure and STM result, the product of UV-light induced molecules should be  $\beta$ -truxinic acid, indicating a dimerization on AOCA molecules on the Au(111) surface. From the chemical structure of a dimer, spot 2 could be ascribed to two carboxyl groups. The other two spots, 1 and 3, are ascribed to the phenyl

rings with alkyl chains. The AOCA dimers in a pair adopt opposite orientations as shown in the figure indicated by I and II. On the basis of the STM results, a tentative model for the photochemically resulted dimeric AOCA adlayer is proposed in Figure 4c, in which a  $(5 \times 8)$  unit cell is outlined.

It is noted that AOCA has not been dimerized completely after illumination for less than 10 min. In the STM image shown in Figure 5, two molecular domains can be recognized clearly. In domain B, the packing pattern is the same as that in Figure 3, corresponding to an AOCA monomer SAM without dimerization. In domain A, the molecular arrangement is identical with that observed in Figure 4, indicating the adsorption of the AOCA dimers. This image has directly demonstrated the photochemical reaction on Au(111) surface and resulted structural transformation of molecular arrangement in the two SAMs.

**FT-IR Spectroscopy.** To confirm the occurrence of photo-dimerization, FT-IR was carried out to study the molecular structure. The AOCA (4-(amyloxy)cinnamic acid) was dissolved in ethanol. Those samples for FT/IR measurement were prepared by dropping the AOCA solution to a gold-covered silicon plate.

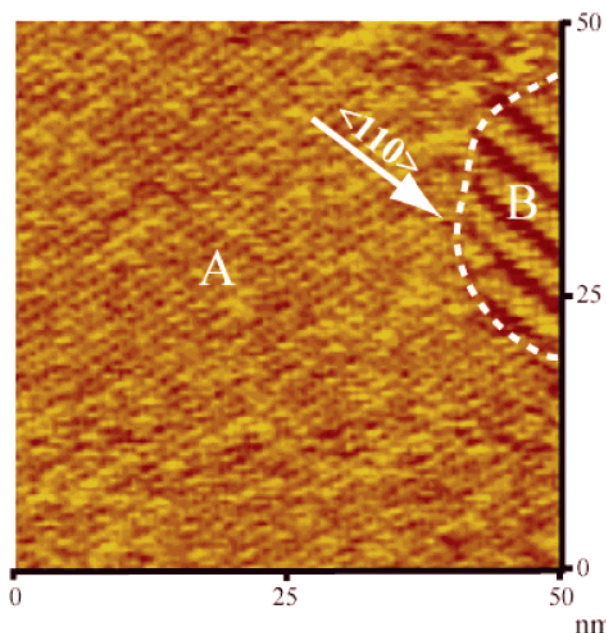


**Figure 5.** STM image of the AOCA adlayer consisting of two domains. Domain A corresponds to dimerized area and B undimerized area. The bias voltage and tunneling current were  $-100$  mV and  $+700$  pA, respectively.

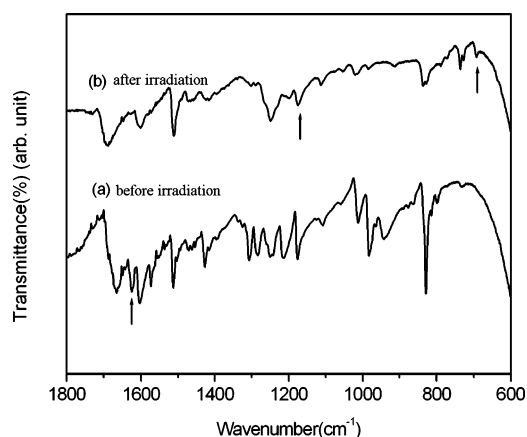


**Figure 6.** Infrared spectra of AOCA-modified gold film: (a) before irradiation; (b) after irradiation.

The IR spectra of AOCA before (a) and after the irradiation (b) are shown in the Figure 6 and compared with the results in the literature.<sup>25,26</sup> The aliphatic C=C stretching mode at  $1625\text{ cm}^{-1}$  is changed from strong to weak after UV-light irradiation. The new band at  $1170\text{ cm}^{-1}$  in Figure 4b is associated with cyclobutane ring stretching vibration. Another band appeared at  $691\text{ cm}^{-1}$  after irradiation is assigned to the cyclobutane ring deformation. These results confirm the photodimerization by cyclobutane ring formation. The band at  $1666\text{ cm}^{-1}$  before irradiation is the C=O stretching mode. After the irradiation, this band is moved to  $1690\text{ cm}^{-1}$ , which is possibly due to the loss of conjugation and the disruption of hydrogen bonds after dimerization.<sup>25,26</sup>

According to the classic topochemical principle, the double bonds of neighboring molecules in a crystal should arrange in a parallel fashion and make contact at a distance of  $4.2\text{ Å}$  or less.<sup>27</sup> But in the present AOCA monomer SAM, the molecular distance is fairly larger ( $6.0\text{ Å}$ ). As described by Ramamurthy and Venkatesan, the concepts of “reaction cavity” and “dynamic preformation” have refined the original “topochemical principles”.<sup>28,29</sup> A reaction that may not be expected on the basis

of the ground-state structure may indeed occur if the dynamic preformation can be tolerated in the crystal lattice by the nearest neighbors.<sup>14,20</sup> Photoexcitation create short-term lattice instability, which drives one molecule close to a neighbor and give the molecule a more favorable orientation so as to cause a photochemical reaction. As for AOCA SAMs, short-term lattice instability can be caused by photoexcitation. Electronic excitation increases the attractive forces. Therefore, the excited molecule is bound more tightly to its neighbor and the maximum overlap geometry may be expected. Then the photodimerization does take place in the monolayer.

## Conclusion

In summary, the SAM of AOCA on Au(111) surface has been fabricated and investigated by CV, ECSTM and FT-IR. High-resolution STM images reveal the details of the molecular arrangements. A well-ordered SAM is prepared on Au(111) before UV light irradiation. After the UV light irradiation, a dimeric structure with regular molecular rows is observed. The results show that the molecular arrangement and packing symmetry of AOCA adlayer can be easily tuned by photochemical reaction. The direct evidence of photodimerization of cinnamic acid on metal substrate at molecular level is provided. The results will be important in nanostructure construction and development of photoresponsive electric nanodevices.

**Acknowledgment.** This work was supported by the National Natural Science Foundation of China (No. 20025308, 20177025, and 20121301), National Key Project on Basic Research (Grants G2000077501 and 2002CCA03100) and Chinese Academy of Science. Xu thanks Prof. C. L. Bai for discussion.

## References and Notes

- (1) *Molecular Electronics*; Jortner, J., Ratner, M., Eds.; IUPAC Chemistry for the 21st Century Monographs; Blackwell Science: Oxford, U.K., 1997.
- (2) Joachim, C.; Gimzewski, J. K.; Aviram, A. *Nature* **2000**, *408*, 541.
- (3) Xu, S.; Szymanski, G.; Lipkowski, J. *J. Am. Chem. Soc.* **2004**, *126*, 12276.
- (4) Yamada, R.; Wano, H.; Uosaki, K. *Langmuir* **2000**, *16*, 5523.
- (5) Wandlowski, T. H.; Hölzle, M. H. *Langmuir* **1996**, *12*, 6604.
- (6) Wan, L. J.; Noda, H.; Wang, C.; Bai, C. L.; Osawa M. *Chem. Phys. Chem.* **2001**, *617*.
- (7) Mougous, J. D.; Brackley, A. J.; Foland, K.; Baker, R. T.; Patrick, D. L. *Phys. Rev. Lett.* **2000**, *84*, 2742.
- (8) Li, W.; Lynch, V.; Thompson, H.; Fox, M. A. *J. Am. Chem. Soc.* **1997**, *119*, 7211.
- (9) Abbott, S.; Ralston, J.; Reynolds, G.; Hayes, R. *Langmuir* **1999**, *15*, 8923.
- (10) Itoh, K.; Yamamoto, M.; Furuyama, N.; Saito, A. *Mikrochim Acta* **1997**, *14*, 33.
- (11) Fujii, S.; Akiba, U.; Fujihira, M. *Chem. Commun.* **2001**, *17*, 1688.
- (12) Yoshimoto, S.; Tsutsumi, E.; Honda, Y.; Murata, Y.; Murata, M.; Komatsu, K.; Ito, O.; Itaya, K. *Angew. Chem., Int. Ed. Engl.* **2004**, *43*, 3044.
- (13) Vanoppen, P.; Grim, P. C. M.; Rücker, M.; De Feyter, S.; Moessner, G.; Valiyaveetil, S.; Müllen, K.; De Schryver, F. C. *J. Phys. Chem.* **1996**, *100*, 19636.
- (14) Abdel-Mottaleb, M. M. S.; De Feyter, S.; Gesquière, A.; Sieffert, M.; Klapper, M.; Müllen, K.; De Schryver, F. C. *Nano Lett.* **2001**, *1*, 353.
- (15) Okawa, Y.; Aono, M. *Nature* **2001**, *409*, 683.
- (16) Grim, P. C. M.; De Feyter, S.; Gesquière, A.; Vanoppen, P.; Rücker, M.; Valiyaveetil, S.; Moessner, G.; Müllen, K.; De Schryver, F. C. *Angew. Chem., Int. Ed. Engl.* **1997**, *36*, 2601.
- (17) Qiao, Y.-H.; Zeng, Q. D.; Tan, Z. Y.; Xu, S. D.; Wang, D.; Wang, C.; Wan, L. J.; Bai, C. L. *J. Vac. Sci. Technol. B* **2002**, *20*, 2466.
- (18) Takami, T.; Ozaki, H.; Kasuga, M.; Tsuchiya, T.; Mazaki, Y.; Fukushi, D.; Ogawa, A.; Uda, M.; Aono, M. *Angew. Chem., Int. Ed. Engl.* **1997**, *36*, 2755.
- (19) Miura, A.; De Feyter, S.; Abdel-Mottaleb, M. M. S.; Gesquière, A.; Grim, P. C. M.; Moessner, G.; Sieffert, M.; Klapper, M.; Müllen, K.; De Schryver, F. C. *Langmuir* **2003**, *19*, 6474.

- (20) Yang, G. Z.; Wan, L. J.; Zeng, Q. D.; Bai, C. L. *J. Phys. Chem. B* **2003**, *107*, 5116.
- (21) Dilling, W. L. *Chem. Rev.* **1983**, *83*, 1.
- (22) Hasegawa, M. *Chem. Rev.* **1983**, *83*, 507.
- (23) Clavilier, J.; Faure, R.; Guinet, G.; Durand, R. *J. Electroanal. Chem.* **1980**, *107*, 205.
- (24) Hamelin, A.; Stoicoviciu, L.; Chang, S. C.; Weaver, M. J. *J. Electroanal. Chem.* **1991**, *307*, 183.
- (25) Ghosh, M.; Maity, A. K.; Chakrabarti, S.; Misra, T. N. *Proc. Indian Acad. Sci. (Chem. Sci.)*, **1995**, *107*, 149.
- (26) Ghosh, M.; Charkrabarti, S.; Misra, T. N. *J. Phys. Chem. Solids* **1998**, *59*, 753.
- (27) Zimmerman, H. E.; Nesterov, E. E. *Acc. Chem. Res.* **1968**, *1*, 353.
- (28) Gavezzotti, A. *J. Am. Chem. Soc.* **1985**, *107*, 962.
- (29) Ramamurthy, V.; Venkatesan, K. *Chem. Rev.* **1987**, *87*, 433.